V European Conference on Computational Fluid Dynamics
ECCOMAS CFD 2010
J. C. F. Pereira and A. Sequeira (Eds)
Lisbon, Portugal, 14–17 June 2010

INFLUENCE OF THE FOIL THICKNESS ON THE THRUST OF OSCILLATING FOIL

Marco La Mantia[*] and Peter Dabnichki[†]

[*]Department of Low-Temperature Physics, Faculty of Mathematics and Physics,
Charles University in Prague, V Holešovičkách 2, 180 00 Praha 8, Czech Republic
e-mail: lamantia@nbox.troja.mff.cuni.cz

[†]School of Engineering and Materials Science, Queen Mary University of London,
Mile End Road, London E1 4NS, United Kingdom
e-mail: p.dabnichki@qmul.ac.uk

Key words: Unsteady Fluid Mechanics, Propulsion, Flapping Flight, Boundary Element Method

Abstract. *A simulation of harmonically oscillating wing was performed using a Boundary Element Method computer program and the corresponding fluid forces generated by its motion were analysed. A symmetric 4-digit NACA airfoil was used and its maximum thickness was varied in order to assess the effect of changing the foil shape on the generated trust. It was found that with the increase of the thickness, the thrust coefficient per unit of mass C_{Fx} / m_w decreases in magnitude. This result indicates that if the wing mass m_w for this particular airfoil is fixed, its thickness has to be as small as possible in order to maximise the generated thrust. The other important finding is the dependence on the motion frequency (indicated by the Strouhal number St). If the foil thickness is fixed and St increases, C_{Fx} / m_w increases in magnitude too, as reported in the literature for the investigated range of Strouhal number. However, as the foil thickness becomes larger, the motion frequency effect on the generated thrust appears to become less relevant, i.e. the thrust range for a slender foil is larger than that of a thicker one over the same motion frequency range.*

1 INTRODUCTION

The observation of the swimming and flying capabilities of fish and birds started the idea of using oscillating wings as propulsors, e.g. to replace propellers. Related technology applications are being investigated worldwide and a number of theoretical and experimental studies were published over the past decades: the review papers of Rozhdestvensky and Ryzhov [1] and Triantafyllou et al. [2] can introduce the reader to such an active field of research. Moreover, they show that there is yet a lot more to be learned about flapping flight.

The numerical work presented here focuses then on an issue that has not been investigated, the influence of the foil shape on the forces generated by oscillating wing. The unsteady forces are calculated by using a panel method developed by the authors [3,4]. Its main feature is a novel formulation of the unsteady Kutta condition: a finite pressure difference is postulated at the trailing edge of the moving wing to account for the shedding of trailing-edge vortices and resulting thrust-producing jet [5]. Comparisons with published experimental data showed good agreement with the computational results [3,4]. Wind-tunnel experiments were also performed to validate the developed code and test heaving wing propulsion modes [6,7].

The paper is organised as follows: the used unsteady Boundary Element Method is detailed in the next section. The computational results are then presented and the influence of the foil thickness on the generated thrust is finally discussed.

2 NUMERICAL MODEL

A 4-digit NACA symmetric foil [8] of chord c is moving forward at a steady velocity Q_∞ and oscillating harmonically with a heaving motion z, perpendicular to Q_∞, and with a pitch motion γ. Both harmonic motions are defined by sinusoids and their phase angle is set to 90 deg. A relevant parameter of such oscillations is the Strouhal number St. It can be seen as a measure of the motion unsteadiness and is mathematically expressed by the oscillation frequency f (in Hz) multiplied by the width of the wake (assumed equal to two times the heave amplitude z_0) and divided by the mean flow velocity, i.e.

$$St = f \frac{2 z_0}{Q_\infty} = \frac{\omega}{2\pi} \frac{2 z_0}{Q_\infty}, \qquad (1)$$

where the frequency of oscillation ω is in rad/s.

The most significant kinematic parameters used in the study are c=0.1 m, pitch axis position from the foil leading edge $x_{pitch}=c/3$, Q_∞=0.4 m/s, $z_0=3c/4$ and maximum angle of attack α_{max}=15 deg. Figure 1 displays a foil cycle in the inertia frame of reference (x, z) for St=0.3 (pitch amplitude γ_0=28.3 deg and f=0.8 Hz). The foil is a NACA 0012 with a maximum thickness to chord ratio of 0.12. The instantaneous angle of attack is not explicitly related to the initial conditions and the pitch amplitude is determined by the choice of α_{max} [3].

The presented model follows the well-established approach of Katz and Plotkin [9], the flow is assumed incompressible and irrotational and the foil is represented by a finite number N of linear panels. Constant strength distributions of source σ and doublet μ are situated on each panel's collocation point. The flow potential function φ^* at each collocation point is defined as the sum of a local (perturbation) potential φ, related to the unknown doublet strength μ, and a free-stream potential φ_∞, linked to the known fluid kinematic velocity. An internal Dirichlet boundary condition is imposed in order to meet the non-penetration condition. At each foil collocation point the source strength is known, $\sigma=q_k\, n$, where n is a unit vector normal to the foil surface pointing into the foil and q_k the fluid kinematic velocity due to the imposed motion of the foil. The governing

integral equation is derived by using the Laplace's equation and Green's third identity. In the body-fixed coordinate system, at time t and for each foil collocation point it can be written as

$$\frac{1}{2\pi}\int_{S}(\sigma \ln r - \mu\frac{\partial \ln r}{\partial n})\,dS - \frac{1}{2\pi}\int_{S_w}\mu_w\frac{\partial \ln r}{\partial n}\,dS_w = 0\,, \qquad (2)$$

where S and S_w indicate the foil and wake surface, respectively, and μ_w is the strength of the wake doublet distribution. To define uniquely the problem μ_w has to be known or related to the unknown doublets on S by the means of a suitable condition, i.e. the Kutta condition. Besides, S_w changes with time, that is, new portions of the wake surface are added as time advances. Hence the wake shape has to be properly modelled. This can be seen as an additional assumption to in effect represent initial conditions for the dynamic problem.

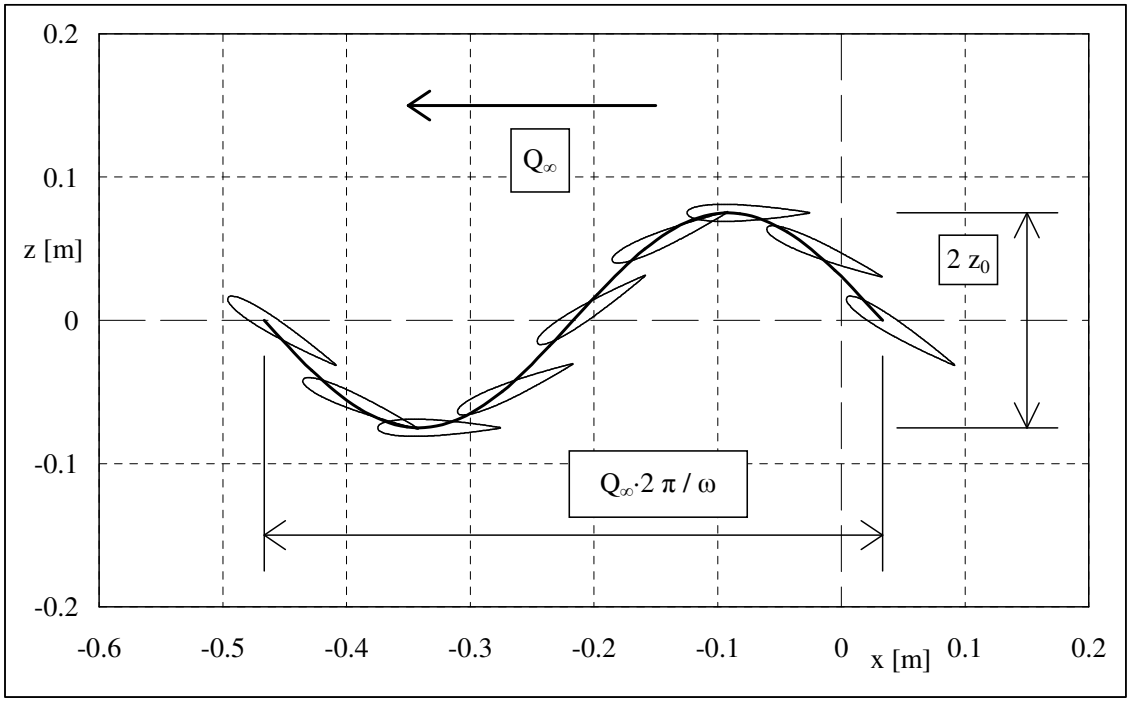

Figure 1: Foil harmonic cycle in the inertia coordinate system for St=0.3.

The discretized form of Equation (2) is

$$\sum_{j=1}^{N} B_j\,\sigma_j + \sum_{j=1}^{N} C_j\,\mu_j + \sum_{l=1}^{M} C_{wl}\,\mu_{wl} = 0\,, \qquad (3)$$

where B_j and C_j are the appropriate two-dimensional source and doublet influence coefficients of panel j at the considered collocation point, respectively: they only depend on the foil geometry [3]. The wake influence coefficient C_{wl} is defined as C_j, i.e. it is just a function of the foil and wake geometries. M indicates the number of linear wake panels at time t (e.g. at the first time step M is equal to 1). At each time step a new wake panel is added and its contribution evaluated. The wake panels are not linked between them, that is, the wake is not continuous and is modelled as discrete doublet panels of constant strength μ_w and assigned length l_w. Besides, the unknowns are N+1 since at time t the doublet strengths of the previously shed wake panels are already derived. The wake panels' positions must also be modelled. Following [4] it was assumed that the wake panels remain where shed in the inertia coordinate system, i.e. the wake follows the foil path (see Figure 1). The body-fixed position of the wake panel

closest to the trailing edge, the one added at each time step, is always set parallel to the chord. The panel's length was set proportional to the time step length times the steady fluid velocity [9].

The trailing-edge condition, necessary to obtain a unique solution, was derived from the unsteady Bernoulli equation, the conservation of momentum equation for incompressible fluid and irrotational flow. It implies that the second derivative of every involved function, such as the fluid velocity and pressure, exists and is continuous (C^2 space). This is not the case everywhere in the considered domain as the airfoil is a C^0 profile with a singularity at the trailing edge.

Following Cebeci et al. [10] the unsteady Bernoulli equation can be written for a generic point on the foil as

$$p_\infty + \frac{1}{2}\rho q_k^2 = p + \frac{1}{2}\rho q^2 + \rho \frac{\partial \varphi^*}{\partial t}, \qquad (4)$$

where p_∞ is the fluid pressure far from the oscillating foil, p the pressure, q the velocity, q_k the kinematic velocity due to the motion of the foil and φ^* the potential function. The fluid velocity is the sum of q_k and the perturbation velocity, which is estimated by the means of the spatial derivative of the perturbation potential φ over the foil. Besides, ρ is the fluid density, which is assumed constant and uniform. In the vicinity of the trailing edge the unsteady Bernoulli equation can be written as

$$p_l + \frac{1}{2}\rho (q_l^2 - q_{k\,l}^2) + \rho \frac{\partial \varphi_l^*}{\partial t} = p_u + \frac{1}{2}\rho (q_u^2 - q_{k\,u}^2) + \rho \frac{\partial \varphi_u^*}{\partial t}, \qquad (5)$$

where the subscripts l and u indicate the collocation points of the lower and upper panels that meet at the trailing edge, respectively. It is important to underline that, as the trailing edge is the domain singularity point, the velocity and pressure can there assume more than one value, that is, a pressure difference can there exist. Equation (5) shows also that the unsteady Bernoulli equation alone is not sufficient to obtain the solution: it is necessary to specify relevant boundary conditions, e.g. the values of velocity or pressure.

It was postulated that the pressure difference at the trailing edge could be finite rather than zero [3-5]. This assumption implies that the energy supplied for the wing motion would generate time-dependant trailing-edge vortices. Their overall effect, which depends on the motion initial parameters, would be a jet of fluid that propels the wing. As the kinetic energy is transferred from the jet back to the wing, the vortical structures would disappear. The postulated pressure difference at the trailing edge is then fundamental for such a model as it can justify the velocity difference that generates the thrust-producing jet.

The devised code assumes incompressible fluid and irrotational flow and evaluates the global potential function φ^* at each time step. These form the sufficient condition to calculate the velocity distribution over the foil in the body-fixed coordinate system, the one moving together with the foil, by estimating the spatial derivative of the potential function over the foil. The subsequent calculation of the pressure coefficient is followed by the evaluation of the centre of pressure acceleration in the inertia frame of reference. The latter is used for the force coefficients calculations. A time-averaged force (as detailed below) is obtained before computing the coefficients: a 0.6 m wing span s and a 300 kg/m^3 wing average density were used (the wing was assumed rectangular). The fluid density ρ was set to 1000 kg/m^3 and its dynamic viscosity to 0.001 Pa s (i.e. water). The Reynolds number resulted then equal to 40,000 for c=0.1 m.

Following Cebeci et al. [10] the pressure coefficient C_p at each foil collocation point and time step is defined as

$$C_p = \frac{p - p_\infty}{\frac{1}{2}\rho Q_\infty^2} = \frac{q_k^2}{Q_\infty^2} - \frac{q^2}{Q_\infty^2} - \frac{2}{Q_\infty^2}\frac{\partial \varphi^*}{\partial t}. \qquad (6)$$

Every pressure coefficient is multiplied by the respective panel length. The x and z body-fixed components of the non-dimensional forces are then calculated to obtain the non-dimensional body-fixed thrust and lift. Such a system of pressure forces acting on the foil can be represented by an equivalent single point force applied at the centre of pressure, which is defined as the point where the total moment is zero. Once the time-dependent position of the centre of pressure is evaluated the time-averaged forces in the x and z directions of the inertia coordinate system can be calculated as

$$\overline{F}_x = m_w\, a_{ref}\, a_x \qquad (7)$$

and

$$\overline{F}_z = m_w\, a_{ref}\, a_z, \qquad (8)$$

where m_w is the wing mass, a_x and a_z are the time-averaged non-dimensional centre of pressure accelerations in the inertia frame of reference and a_{ref} a reference acceleration.

The force coefficients in the x and z directions of the inertia coordinate system, which are also called the thrust and lift coefficients, respectively, are defined as

$$C_{Fx} = \frac{\overline{F}_x}{\frac{1}{2}\rho\, c\, s\, Q_\infty^2} \qquad (9)$$

and

$$C_{Fz} = \frac{\overline{F}_z}{\frac{1}{2}\rho\, c\, s\, Q_\infty^2}. \qquad (10)$$

The thrust coefficient C_{Fx} is negative, if there is thrust, and the lift coefficient C_{Fz} is positive, if there is lift.

3 RESULTS AND DISCUSSION

The 4-digit NACA foil was geometrically approximated by 200 linear panels N. Two hundred time steps were used for each calculation, that is, five complete oscillations and forty time steps N_t for each foil cycle. The time step length Δt is defined as the time length of one harmonic cycle t_{cycle} divided by N_t. The wake panels' length l_w was set proportional to the time step length, i.e. l_w=0.75 $\Delta t\, Q_\infty$ [3,5,9].

In Figure 2 the instantaneous inertia forces generated by the oscillating foil are plotted as a function of non-dimensional time (t/t_{cycle}=1 at the end of the first oscillation) for a sample case: the foil maximum thickness t is again equal to 0.12c, i.e. the foil is a NACA 0012 (the other relevant kinematic parameters are as discussed above).

The force in the x direction of the inertia coordinate system is always negative, i.e. thrust is always present, as expected for a potential model. The time-averaged lift is zero, as the harmonic motion is symmetric with respect to the x axis. It should also be noted that the thrust frequency is twice that of the lift.

Figure 3 displays the pressure coefficient over the foil as a function of the collocation point position in the chord-wise direction of the body-fixed frame of reference, at the last time step of the harmonic motion (the angle of attack is maximum), for the same case as in Figure 2. It can be seen that a finite pressure difference exists at the trailing edge of the oscillating foil, as expected. This overview shows that the obtained general results are physically sound and reliable [3-5,11-14].

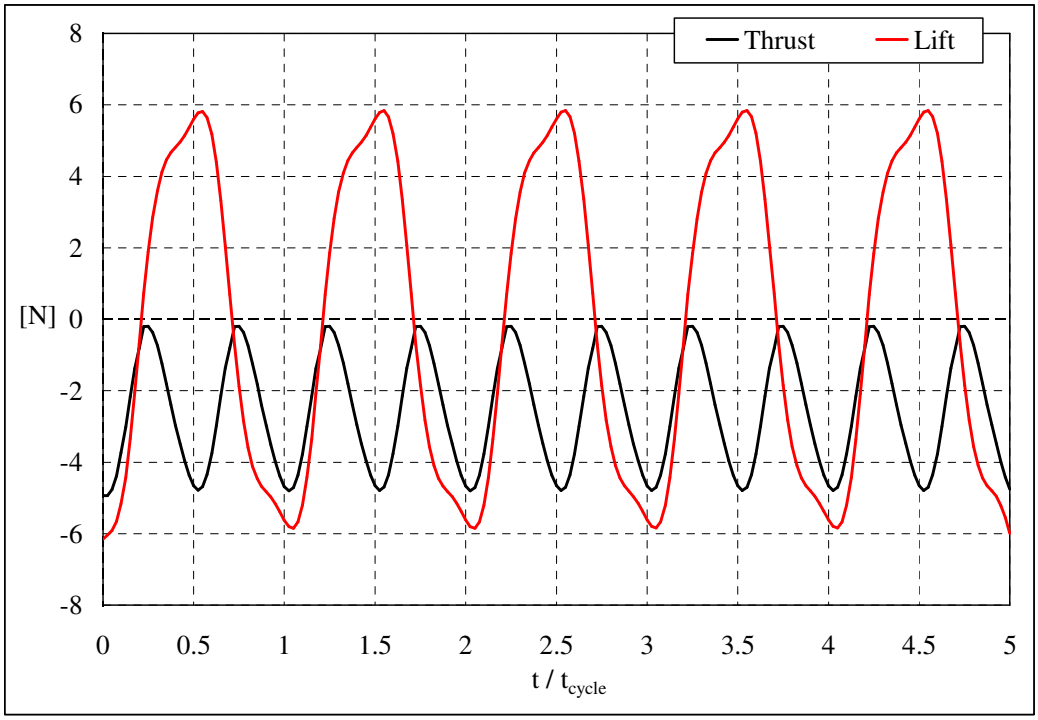

Figure 2: Instantaneous forces in the x and z directions of the inertia coordinate system (the thrust F_x and lift F_z, respectively) as a function of non-dimensional time for St=0.3 and t=0.12c.

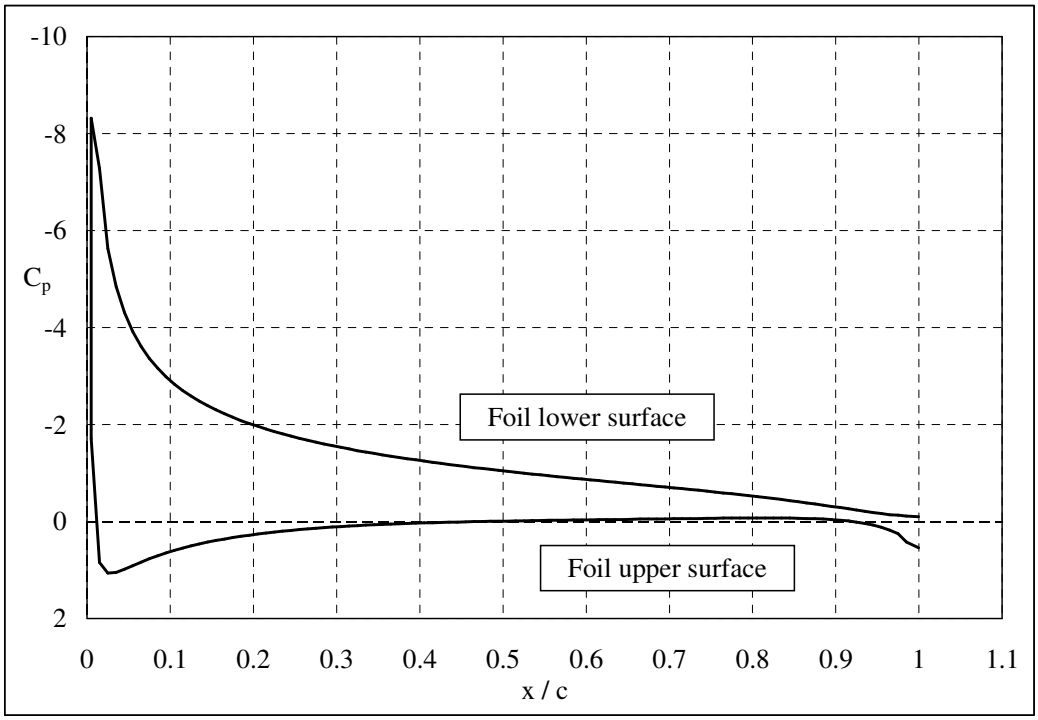

Figure 3: Pressure coefficients at the last time step as a function of the collocation point position in the body-fixed coordinate system for St=0.3 and t=0.12c.

In order to analyse the influence of the foil shape on the generated thrust it was decided to vary its maximum thickness t while preserving the foil geometry classification. The thickness is maximal at one third of the chord for a 4-digit NACA foil. Foils with different maximum thickness in the body fixed frame of reference are plotted in Figure 4 to visualise their different shapes.

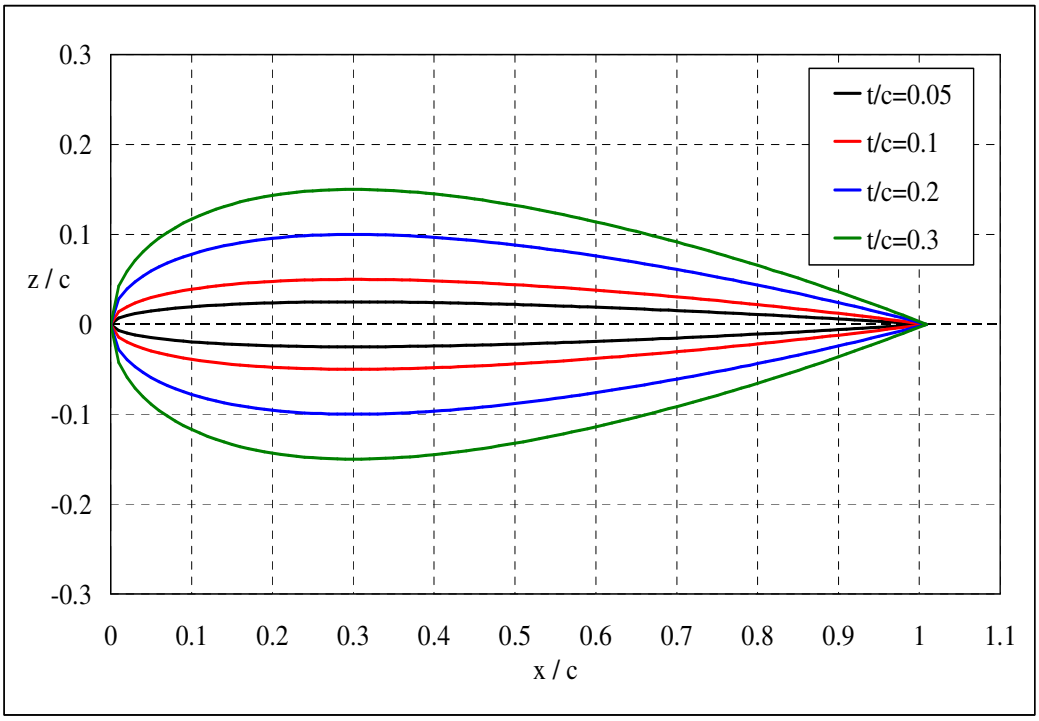

Figure 4: 4-digit NACA airfoils.

Table 1 lists the thrust coefficient as a function of the foil maximum thickness. As t increases, C_{Fx} increases in magnitude. However, the result is not consistent with the observations of natural flyers and swimmers because it does not take properly into account the foil shape. In other words, as the wing mass largely varies with t (see the second column of Table 1), the thrust coefficients as defined by Equation (9) can not be used to compare the performance of such different propulsors.

t / c	m_w [kg]	C_{Fx}		
		St=0.2	St=0.3	St=0.4
0.01	0.012	-0.201	-0.403	-0.694
0.03	0.037	-0.244	-0.453	-0.756
0.06	0.074	-0.281	-0.493	-0.803
0.09	0.111	-0.305	-0.517	-0.827
0.12	0.148	-0.326	-0.537	-0.846
0.15	0.185	-0.346	-0.557	-0.865
0.20	0.246	-0.380	-0.592	-0.883
0.25	0.308	-0.415	-0.630	-0.916
0.30	0.370	-0.451	-0.665	-0.950
0.40	0.493	-0.519	-0.727	-1.012

Table 1: Thrust coefficient as a function of the foil maximum thickness and wing mass for three different values of the Strouhal number.

The ratio C_{Fx} / m_w as a function of the maximum thickness (see Figure 5) provides a better comparison. As t increases, the thrust coefficient per unit of mass decreases in magnitude, that is, if the wing mass is fixed, its thickness has to be as small as possible in order to maximise the generated thrust. This result agrees more closely with the structure of birds wings and fish fins.

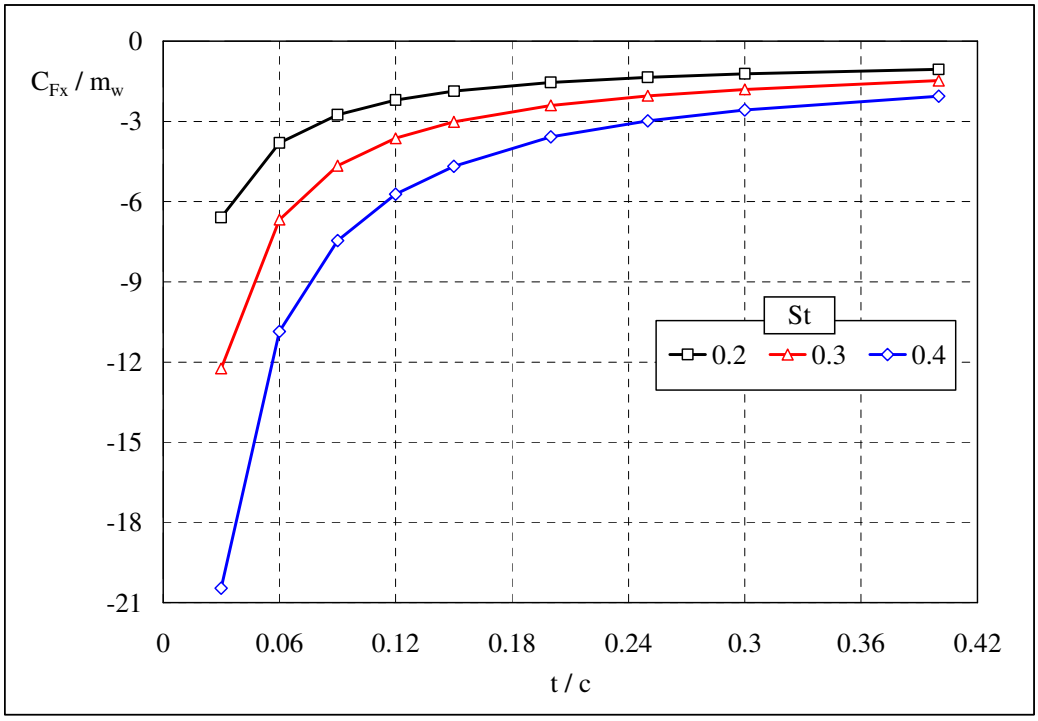

Figure 5: Thrust coefficient per unit of wing mass as a function of the foil thickness for three different values of the Strouhal number.

The influence of the Strouhal number on the generated thrust was also investigated (Table 1 and Figure 5). If the foil thickness is fixed and St increases, C_{Fx} / m_w increases in magnitude. This is supported by results already reported in the literature for the investigated range of Strouhal number (e.g. see [1]). Besides, as the foil thickness becomes larger, the motion frequency effect on the generated thrust appears to be less relevant, that is, the thrust range for a slender foil is larger than that of a thicker one over the same St range. This again points in the direction of slender wings being more effective for propulsion purposes. However, it is important to point out that other parameters influence the forces generated by such propulsors. For example, the added mass has a relevant effect on accelerated motions in water [14-16] and the structural behaviour of the moving wing should also be accounted for when the design of flapping wing is addressed [6,7,14,17].

4 CONCLUSIONS

The computational results presented here show that the foil shape has a noticeable influence on the thrust generated by oscillating wings. To allow a meaningful comparison between different foil shapes the thrust coefficients were normalised using the respective wing masses. Slender wings produce the largest thrust coefficients per unit of mass. Besides, as the foil thickness increases, the motion frequency effect on the generated thrust becomes less relevant, that is, the thrust range for a slender foil is larger than that of a thicker one over the same Strouhal number range. The result agrees with

the observation of natural flyers and swimmers. However, other features of flapping flight, such as the fluid-structure interaction and the added mass effect, are deemed to be significant for a more precise calculation of the generated time-dependent forces. For example, the added mass effect appears to be especially important for bodies accelerating in water as the magnitude and time behaviour of the generated forces largely change, if such an affect is taken into account [15,16]. This is currently being investigated in the case of flapping flight and, once the study is completed, the relevant numerical results will be submitted for publication.

REFERENCES

[1] K.V. Rozhdestvensky and V.A. Ryzhov, Aerohydrodynamics of Flapping-Wing Propulsors. *Prog. Aerosp. Sci.* **39**, pp. 585-633 (2003)

[2] M.S. Triantafyllou, A.H. Techet and F.S. Hover, Review of Experimental Work in Biomimetic Foils. *IEEE J. Oceanic. Eng.* **29**, pp. 585-594 (2004)

[3] M. La Mantia and P. Dabnichki, Unsteady Panel Method for Flapping Foil. *Eng. Anal. Bound. Elem.* **33**, pp. 572-580 (2009)

[4] M. La Mantia and P. Dabnichki, Unsteady 3D Boundary Element Method for Oscillating Wing. *CMES-Comp. Model. Eng.* **33**, pp. 131-153 (2008)

[5] M. La Mantia and P. Dabnichki, Influence of the Wake Model on the Thrust of Oscillating Foil. Submitted (2009)

[6] M. La Mantia and P. Dabnichki, Numerical and Experimental Analysis of Oscillating Wing, In proceedings of the *4th Symposium on Integrating CFD and Experiments in Aerodynamics*, Von Karman Institute for Fluid Dynamics, Rhode-St-Genèse, Belgium, in print (2009)

[7] M. La Mantia and P. Dabnichki, Experimental Analysis of Heaving Wing, In proceedings of the *International Conference Experimental Fluid Mechanics 2009*, T. Vit, P. Dančová and V. Dvořák Eds., Liberec, Czech Republic, pp. 157-167 (2009)

[8] I.H. Abbott and A.E. Von Doenhoff, Theory of Wing Sections, Dover Publications (1959)

[9] J. Katz and A. Plotkin, Low-Speed Aerodynamics, 2nd edition, Cambridge University Press (2001)

[10] T. Cebeci, M. Platzer, H. Chen, K.-C. Chang and J.P. Shao, Analysis of Low-Speed Unsteady Airfoil Flows, Springer (2005)

[11] D.R. Poling and D.P. Telionis, The Response of Airfoils to Periodic Disturbances - The Unsteady Kutta Condition. *AIAA J.* **24**, pp. 193-199 (1986)

[12] J. Young and J.C.S. Lai, Oscillation Frequency and Amplitude Effects on the Wake of a Plunging Airfoil. *AIAA J.* **42**, pp. 2042-2052 (2004)

[13] R. Liebe, Unsteady Flow Mechanisms on Airfoils: the Extended Finite Vortex Model with Applications, In *Flow Phenomena in Nature - Volume 1: A Challenge to Engineering Design*, R. Liebe Ed., WIT Press, pp. 283-339 (2005)

[14] M. La Mantia, Analysis of Hydrodynamic Forces on Flapping Wing, PhD Thesis, Queen Mary University of London (2009)

[15] P. Gardano and P. Dabnichki**,** Application of Boundary Element Method to Modelling of Added mass and its Effect on Hydrodynamic Forces. *CMES-Comp. Model. Eng.* **15**, pp. 87-98 (2006)

[16] P. Gardano and P. Dabnichki**,** On Hydrodynamics of Drag and Lift of the Human Arm. *J. Biomech.* **39**, pp. 2767-2773 (2006)

[17] P. Dabnichki and M. La Mantia, Dynamic Loads and Strength Requirements for Flapping Wing. *Key Eng. Mat.* **348-349**, pp. 945-948 (2007)